1521-0111/12/8206-1136–1149$25.00
MOLECULAR PHARMACOLOGY
Vol. 82, No. 6
80507/3805834
Copyright © 2012 The American Society for Pharmacology and Experimental Therapeutics
Mol Pharmacol 82:1136–1149, 2012

Gβγ Inhibits Exocytosis via Interaction with Critical Residues on Soluble *N*-Ethylmaleimide-Sensitive Factor Attachment Protein-25

Christopher A. Wells, Zack Zurawski, Katherine M. Betke, Yun Young Yim, Karren Hyde, Shelagh Rodriguez, Simon Alford, and Heidi E. Hamm

Department of Pharmacology, Vanderbilt University Medical Center, Nashville, Tennessee (C.A.W., Z.Z., K.M.B., Y.Y.Y., K.H., H.E.H.); and Department of Biological Sciences, University of Illinois at Chicago, Chicago, Illinois (S.R., S.A.)

Received June 8, 2012; accepted September 7, 2012

ABSTRACT

Spatial and temporal regulation of neurotransmitter release is a complex process accomplished by the exocytotic machinery working in tandem with numerous regulatory proteins. G-protein βγ dimers regulate the core process of exocytosis by interacting with the soluble *N*-ethylmaleimide-sensitive factor attachment protein receptor (SNARE) proteins soluble *N*-ethylmaleimide-sensitive factor attachment protein-25 (SNAP-25), syntaxin 1A, and synaptobrevin. Gβγ binding to ternary SNAREs overlaps with calcium-dependent binding of synaptotagmin, inhibiting synaptotagmin-1 binding and fusion of the synaptic vesicle. To further explore the binding sites of Gβγ on SNAP-25, peptides based on the sequence of SNAP-25 were screened for Gβγ binding. Peptides that bound Gβγ were subjected to alanine scanning mutagenesis to determine their relevance to the Gβγ-SNAP-25 interaction. Peptides from this screen were tested in protein-protein interaction assays for their ability to modulate the interaction of Gβγ with SNAP-25. A peptide from the C terminus, residues 193 to 206, significantly inhibited the interaction. In addition, Ala mutants of SNAP-25 residues from the C terminus of SNAP-25, as well as from the amino-terminal region decreased binding to $G\beta_1\gamma_1$. When SNAP-25 with eight residues mutated to alanine was assembled with syntaxin 1A, there was significantly reduced affinity of this mutated t-SNARE for Gβγ, but it still interacted with synaptotagmin-1 in a Ca^{2+}-dependent manner and reconstituted evoked exocytosis in botulinum neurotoxin E-treated neurons. However, the mutant SNAP-25 could no longer support 5-hydroxytryptamine-mediated inhibition of exocytosis.

Introduction

Release of neurotransmitter into the synapse is a complex, regulated process involving core exocytotic machinery proteins, accessory proteins that play roles in docking and priming the vesicle, ion channels, calcium sensors, and presynaptic inhibitory G-protein-coupled receptors (GPCRs). Previous studies over the past 20 years have shown that the Gβγ subunit, part of the heterotrimeric G-protein complex activated by GPCRs, has a variety of effectors that it can interact with and regulate when dissociated from Gα upon GPCR activation (Clapham and Neer, 1997; Gautam et al., 1998; Vanderbeld and Kelly, 2000; Cabrera-Vera et al., 2003; Blackmer et al., 2005; Gerachshenko et al., 2005; Smrcka, 2008). In the presynapse, Gβγ has been shown to be an important regulator of neurotransmission through interactions with calcium channels (Hille, 1994; Ikeda and Dunlap, 1999; Dolphin, 2003) and with the secretory machinery itself (Blackmer et al., 2001, 2005; Gerachshenko et al., 2005; for review, see Betke et al., 2012). In particular, Gβγ binds directly to the ternary SNARE complex (a trimer of SNAP-25, syntaxin 1A, and synaptobrevin), as established in biochemical as well as in vitro assays (Blackmer et al., 2001, 2005; Gerachshenko et al., 2005; Photowala et al., 2006; Delaney et al., 2007; Yoon et al., 2007, 2008; Zhao et al., 2010; Zhang et al., 2011).

The first (Blackmer et al., 2001) insight into a direct interaction between Gβγ and SNARE proteins was derived from

This work was supported by the National Institutes of Health National Eye Institute [R01-EY010291]; the National Institutes of Health National Center for Research Resources [UL1-RR024975-01]; and the National Institutes of Health National Heart, Lung, and Blood Institute [T32-HL007411].

Article, publication date, and citation information can be found at http://molpharm.aspetjournals.org.

http://dx.doi.org/10.1124/mol.112.080507.

ABBREVIATIONS: GPCR, G-protein-coupled receptor; SNARE, soluble *N*-ethylmaleimide-sensitive factor attachment protein receptor; SNAP, soluble *N*-ethylmaleimide-sensitive factor attachment protein; BoNT/A, botulinum neurotoxin A; t-SNARE, target SNARE; GST, glutathione transferase; TBS, Tris-buffered saline; RT, room temperature; TFA, trifluoroacetic acid; HPLC, high-performance liquid chromatography; MIANS, 2-(4′-maleimidylanilino)naphthalene-6-sulfonic acid; BoNT/E, botulinum neurotoxin E; 5-HT, 5-hydroxytryptamine; CI, confidence interval; EPSC, excitatory postsynaptic current; PDB, Protein Data Bank.

studies using botulinum neurotoxin A (BoNT/A) (Blackmer et al., 2001). BoNT/A cleaves the C-terminal nine amino acids from SNAP-25 (Schiavo et al., 1993; Binz et al., 1994). Treatment of presynaptic reticulospinal neurons with BoNT/A disrupted the ability of serotonin to inhibit excitatory postsynaptic action potentials (Gerachshenko et al., 2005). Furthermore, a 14-amino acid peptide based on the C terminus of SNAP-25 was able to block Gβγ-mediated inhibition (Blackmer et al., 2005; Gerachshenko et al., 2005). Reductions in binding between Gβγ and BoNT/A-cleaved SNAP-25 compared with uncleaved SNAP-25 confirmed the importance of the Gβγ-SNAP-25 interaction (Yoon et al., 2007; Zhao et al., 2010). In addition to binding to SNAP-25, Yoon et al. (2007) showed that Gβγ also binds individually to the other SNARE proteins, syntaxin 1A and synaptobrevin, as well as to the t-SNARE dimer (SNAP-25 with syntaxin 1A) and to the ternary SNARE complex. This mechanism of Gβγ-mediated inhibition of secretion has been identified in neurons (Blackmer et al., 2001; Delaney et al., 2007; Zhang et al., 2011), chromaffin cells (Yoon et al., 2008), and pancreatic β-cells (Zhao et al., 2010).

The specific binding sites on each of the component proteins of the Gβγ-SNARE interaction have yet to be determined. Removal of the C-terminal 26 residues of SNAP-25 (Yoon et al., 2007) disrupted its interaction with Gβγ. In this article, we have mapped the binding sites involved in the interaction of Gβγ with SNAP-25 using peptides of 15 amino acids that cumulatively span the full-length sequence of SNAP-25 for interaction with $G\beta_1\gamma_1$. We found eight residues in SNAP-25 that were important for binding $G\beta_1\gamma_1$. By mutating the corresponding residues in full-length SNAP-25, we found a decreased interaction with fluorescently labeled $G\beta_1\gamma_1$. This mutant SNAP-25, when introduced into lamprey neurons, was no longer able to mediate the effect of 5-HT on presynaptic inhibition of exocytosis.

Materials and Methods

Plasmids. The open reading frame for SNAP-25 was subcloned into the glutathione transferase (GST) fusion vector pGEX-6p-1 (GE Healthcare, Chalfont St. Giles, Buckinghamshire, UK) for expression in bacteria. Mutagenesis of SNAP-25 was accomplished via the overlapping primer method. The SNAP-25 (8A) mutant was subcloned from pGEX-6p-1 into the pRSFDuet-1 plasmid, a dual-expression vector that contains cDNAs for both full-length syntaxin 1A and SNAP-25 that results in concomitant expression and formation of t-SNARE complexes (kindly provided by E. Chapman, University of Wisconsin, Madison, WI). Plasmids were verified to contain the desired mutations via Sanger sequencing using BigDye Terminator dyes and resolved on an ABI 3730 DNA Analyzer (Applied Biosystems, Foster City, CA).

Antibodies. The antibody for rabbit Gβ (T-20) was obtained from Santa Cruz Biotechnology, Inc. (Santa Cruz, CA). The horseradish peroxidase-conjugated goat anti-rabbit antibody was obtained from PerkinElmer Life and Analytical Sciences (Waltham, MA). The anti-synaptotagmin-1 antibody subclone 41.1 was obtained from Synaptic Systems GmbH (Goettingen, Germany). Anti-GST (goat) antibody DyLight 800 Conjugated and anti-mouse IgG (goat, H&L) antibody IRDye700DX Conjugated Preadsorbed were both from Rockland Immunochemicals (Gilbertsville, PA).

SNAP-25 Protein Purification. Recombinant bacterially expressed GST fusion proteins were expressed in *Escherichia coli* strain Rosetta 2 (EMD Biosciences, San Diego, CA). Protein expression was induced with 100 μM isopropyl β-D-1-thiogalactopyranoside for 16 h at room temperature. Bacterial cultures were pelleted and washed once with phosphate-buffered saline before undergoing resuspension in lysis buffer (HEPES-KOH, pH 8.0, 150 mM KCl, 5 mM 2-mercaptoethanol, 10.66 μM leupeptin, 1.536 μM aprotinin, 959 nM pepstatin, 200 μM phenylmethylsulfonyl fluoride, and 1 mM EDTA). Cells were lysed with a sonic dismembranator at 4°C for 5 min. Lysates were cleared via ultracentrifugation at 26,000*g* for 20 min in a TI-70 rotor (Beckman Coulter, Fullerton, CA). GST-SNAP-25 fusion proteins were purified from cleared lysates by affinity chromatography on GE Sepharose 4 FastFlow (GE Healthcare). Lysates were allowed to bind to resin overnight before being washed once with lysis buffer containing 1% Triton X-100 (Dow Chemical, Midland, MI). The resin was then washed once with elution buffer (25 mM HEPES-KOH, pH 8.0, 150 mM KCl, 5 mM 2-mercaptoethanol, 0.5% *n*-octyl glucoside, 1 mM EDTA, and 10% glycerol). SNAP-25 proteins were eluted from GST fusion proteins immobilized on resin via proteolytic cleavage with a GST-tagged fusion of rhinovirus 3C protease. Protein concentrations were determined with a Bradford assay kit (Thermo Fisher Scientific, Waltham, MA), and purity was verified by SDS-polyacrylamide gel electrophoresis analysis.

t-SNARE Protein Purification. For the t-SNARE with full-length syntaxin with SNAP-25, this was expressed using the tandem vector (pRSFDuet-1) characterized previously by Chicka et al. (2008). This SNAP-25-syntaxin 1A dimer was purified as described previously (Tucker et al., 2004) using a 6xHis tag present on the N terminus of SNAP-25. After elution, the t-SNARE was dialyzed into a final buffer consisting of 25 mM HEPES-KOH, pH 8.0, 50 mM NaCl, 5 mM 2-mercaptoethanol, 0.5% *n*-octyl glucoside, and 5% glycerol. The *n*-octyl glucoside was used to prevent aggregation that may occur because of the hydrophobic transmembrane domain of syntaxin 1A that is present in this construct. After dialysis, the purified t-SNARE was divided into aliquots and frozen at −80°C.

Gβγ Purification. $G\beta_1\gamma_1$ was purified from bovine retina as described previously (Mazzoni et al., 1991). Recombinant $G\beta_1\gamma_2$ was expressed in Sf9 cells and purified via a 6xHis tag on $G\gamma_2$ using Talon immobilized metal affinity chromatography (Clontech, Mountain View, CA).

Peptide Array Synthesis. Peptide array synthesis was performed using the ResPep SL peptide synthesizer (Intavis AG, Koeln, Germany) according to standard SPOT synthesis protocols (Frank, 2002; Eaton et al., 2008). In brief, the robotics-driven computer-directed device (ResPep SL) managed complex timing, mixing, additions, and washing of the membrane over the course of the peptide synthesis. Peptides were 15 residues in length. The sequences of the peptides for SNAP-25 were based on the sequence available from the UniProtKB/Swiss-Prot database for human SNAP-25 (P60880). After the peptides were synthesized coupled to the membranes, membranes were processed with a final side chain deprotection step. Membranes were placed in an acid-safe container in a chemical hood and submerged in a solution of 95% trifluoroacetic acid and 3% triisopropylsilane for 1 h with intermittent agitation. After the trifluoroacetic acid solution was removed, the membrane was then put through a series of washes: 1) dichloromethane for four 10-min washes; 2) dimethylformamide for four 10-min washes; and 3) ethanol for two 2-min washes. The membrane was allowed to dry in the hood. For the alanine mutagenesis screening of peptides, the peptides were synthesized to be 14 residues in length.

Peptide Membrane Far-Western Blots. After membranes had dried from the synthesis deprotection washes, they were first soaked in ethanol for 5 min and then were rehydrated over two washes for 5 min in water. The membranes were then blocked with slight agitation for 1 h in a buffer of Tris-buffered saline (TBS) with 5% milk and 0.1% Tween 20 (Sigma-Aldrich, St. Louis, MO) and washed five times for 5 min in TBS with 0.1% Tween 20 on a shaker at room temperature (RT). The membranes were then incubated overnight at 4°C with $G\beta_1\gamma_1$ at a final concentration of 0.44 μM in a binding buffer of 20 mM HEPES, pH 7.5, and 5% glycerol. The next morning, membranes were washed at RT on a shaker three times for 5 min in TBS with 5% milk and 0.1% Tween 20. Membranes were then ex-

posed to primary antibody against Gβ at 1:5000 dilution in TBS with 0.2% Tween 20 by mixing on a shaker table at RT for 1 h before being washed three times for 5 min each on a shaker table in TBS with 0.1% Tween 20 also at RT. The appropriate secondary antibody was then diluted into TBS to 1:10,000 dilution with 5% milk and 0.2% Tween 20 followed by gentle agitation on a shaker with membranes for 1 h at RT. Finally, membranes were washed twice for 5 min in TBS with 0.1% Tween 20, followed by two 10-min washes in TBS at RT.

Chemiluminescence. The Western Lightning Chemiluminescence Reagent Plus from Perkin-Elmer Life and Analytical Sciences and the Immun-Star WesternC Chemiluminescence Kit from Bio-Rad Laboratories (Hercules, CA) were used to visualize Western blots following published protocols. Western blot images were obtained using a Bio-Rad Gel Doc Imager. Images were analyzed for densitometry using ImageJ (available from http://rsbweb.nih.gov/ij/index.html). Analysis of variance calculations comparing alanine mutant peptide spot intensity with wild-type peptide reactivity were made using GraphPad Prism4 software (version 4.03 for Windows; GraphPad Software, Inc., San Diego, CA).

Peptide Synthesis. Peptides were synthesized with the ResPep SL using TentaGel amide resin as the solid support for standard Fmoc/HBTU chemistry. After the last round of synthesis, the peptides on the columns were treated with 5% acetic anhydride in dimethylformamide to acetylate the N terminus of the peptides. After washing with dimethylformamide followed by chloromethane and overnight drying, the peptides were cleaved from the resin over the course of 3 to 4 h using a mixture of 92.5% trifluoroacetic acid (TFA) and 5% triisopropylsilane with gentle mixing. The peptides dissolved in the TFA mixture were precipitated using ice-cold *tert*-butyl methyl ether. After spinning and overnight drying, the peptides were dissolved either in water or a mixture of water with acetonitrile or 0.1% TFA. The dissolved peptides were snap-frozen in an ethanol-dry ice bath followed by overnight evaporation in a vacuum-assisted evaporative centrifuge with a cold trap (CentriVap; Labconco, Kansas City, MO). Samples were resolubilized in a mixture of water-acetonitrile-0.1% TFA and subjected to preparative HPLC (Gilson, Middleton, WI) on a reverse-phase C18 column (Luna, 30 × 50 mm; Phenomenex, Torrance, CA) at 50 ml/min with a 10 to 90% acetonitrile in water gradient with 0.1% TFA over 5 min. Samples were then subjected to liquid chromatography/mass spectrometry (Agilent 1200 LCMS; Agilent Technologies, Santa Clara, CA) for purity and mass spectrometric identification of the peptide. HPLC fractions were evaporated to retrieve the peptide of interest.

Gβγ Labeling. Fluorescence labeling of $G\beta_1\gamma_1$ and binding assays were conducted as described previously (Phillips and Cerione, 1991). In brief, purified $G\beta_1\gamma_1$ was exchanged via a Centricon 10,000 molecular weight concentrator into labeling buffer (20 mM HEPES, pH 7.4, 5 mM $MgCl_2$, 150 mM NaCl, and 10% glycerol) and then was mixed with 2-(4′-maleimidylanilino)naphthalene-6-sulfonic acid (MIANS) in a 5-fold molar excess. The reaction proceeded for 3 h at 4°C before quenching with 5 mM 2-mercaptoethanol. The MIANS-$\beta_1\gamma_1$ complex was separated from unreacted MIANS using a PD-10 desalting column (GE Healthcare). MIANS-$G\beta_1\gamma_1$ was stored in aliquots at −80°C.

Fluorescence Binding. All fluorescence measurements were performed in a fluorescence spectrophotometer (Cary Eclipse; Varian, Inc., Palo Alto, CA) at 17°C. MIANS-$G\beta_1\gamma_1$ was diluted into 0.1 ml of assay buffer (20 mM HEPES, pH 7.5, 5 mM $MgCl_2$, 1 mM dithiothreitol, 100 mM NaCl, 1 mM EDTA, and 0.5% *n*-octyl glucoside) to a final concentration of 20 nM. This assay buffer included 0.5% *n*-octyl glucoside to limit aggregation of the t-SNARE complexes, which contain full-length t-SNARE that includes the hydrophobic transmembrane domain of syntaxin 1A. The MIANS fluorescence was monitored with excitation at 322 nm and emission at 417 nm. Fluorescence changes caused by the addition of SNARE complexes to MIANS-$G\beta_1\gamma_1$ were monitored continuously. The amplitude of the fluorescence reflects the specific site on fluorescently labeled Gβγ and its interaction with each protein. There was no nonspecific binding of the free probe to the SNARE proteins, and MIANS-Gβγ was resistant to photobleaching under experimental conditions (data not shown). The EC_{50} concentrations were determined by sigmoidal dose-response curve fitting with variable slope.

GST Pulldown Assay. Five micrograms of each GST-SNAP-25 protein immobilized on glutathione-Sepharose resin was incubated with a 400 μM concentration of the C2AB domain of synaptotagmin-1 (residues 96–422) for 1 h at 4°C and washed three times with assay buffer (20 mM HEPES, pH 7.0, 80 mM KCl, 20 mM NaCl, and 0.1% *n*-octyl glucoside) in a 1.5-ml Eppendorf tube. Immobilized protein complexes were then transferred to a second 1.5-ml Eppendorf tube to reduce nonspecific binding. The complex was eluted with 20 μl of SDS sample buffer followed by separation via SDS-polyacrylamide gel electrophoresis. Precipitated Gβ was detected via Western blot with a rabbit anti-Gβ antibody. Precipitated synaptotagmin-1 C2AB was detected via Western blot using a mouse anti-synaptotagmin-1 antibody (subclone 41.1; Synaptic Systems GmbH). Western blots were imaged with labeled secondary antibodies: anti-GST (goat) antibody DyLight 680 Conjugated and mouse IgG (H&L) Antibody IRDye700DX Conjugated using the LI-COR Odyssey imager (LI-COR Biosciences, Lincoln, NE).

Electrophysiology and Microinjections. Experiments were performed on isolated spinal cords or spinal cords and brainstems of lampreys (*Petromyzon marinus*). The animals were anesthetized with tricaine methanesulfonate (100 mg/l; Sigma-Aldrich) and sacrificed by decapitation, and the spinal cord was dissected in a ice-cold saline solution (Ringer's) of the following composition: 100 mM NaCl, 2.1 mM KCl, 2.6 mM $CaCl_2$, 1.8 mM $MgCl_2$, 4 mM glucose, and 5 mM HEPES, adjusted to a pH of 7.60. Procedures conformed to institutional guidelines (University of Illinois at Chicago Animal Care Committee).

Paired cell recordings were made between reticulospinal axons and neurons of the spinal ventral horn. Axons of reticulospinal neurons were recorded with sharp microelectrodes containing 1 M KCl, 5 mM HEPES buffered to pH 7.2 with KOH, and a SNAP-25 and BoNT/E mixture as defined below. Electrode impedances ranged from 20 to 50 MΩ. Postsynaptic neurons were recorded with a patch clamp in voltage-clamp conditions. Patch electrodes contained 102.5 mM cesium methane sulfonate, 1 mM NaCl, 1 mM $MgCl_2$, 5 mM EGTA, and 5 mM HEPES, pH adjusted to 7.2 with CsOH.

BoNt/E and proteins were pressure microinjected through presynaptic microelectrodes using a Picospritzer II. Presynaptic recordings were made within 100 μm of the synaptic contact to ensure protein diffusion to the region of the terminal, and this was confirmed by injection of fluorescently tagged SNAP-25 protein in separate experiments. Light-chain BoNT/E (65 μg/ml; List Biological Laboratories Inc., Campbell, CA) was stored at −20°C in 20 mM HEPES, 50 mM NaCl, and 0.015 mM bovine serum albumin at pH 7.4. The buffered toxin was diluted as 5 μl with 20 μl of 2 M $KMeSO_4$ and 5 mM HEPES and 20 μl of solution containing one of three different variants of SNAP-25. SNAP-25 proteins were stored at −20°C in a buffer containing 25 mM HEPES-KOH, pH 8.0, 150 mM KCl, 5 mM 2-mercaptoethanol, 0.5% *n*-octyl glucoside, 1 mM EDTA, and 10% glycerol. The buffered protein mixed with BoNT/E where appropriate was diluted 1:5 with 2 M $KMeSO_4$ and 5 mM HEPES. Microinjections of buffer solutions do not affect the synaptic response or 5-HT inhibition.

Protein Structure Visualization. All representatives of protein structure were made using the computer program PyMOL (Schrödinger, 2010).

Statistics and Curve-Fitting. All statistical analysis (Student's *t* test) and curve-fitting (sigmoidal dose-response with variable slope) were performed using GraphPad Prism.

Results

Screening of SNAP-25 Peptides for Interaction with Gβγ. Removal of various portions of the C terminus of SNAP-25 diminished or disrupted binding between Gβγ and SNAP-25 (Yoon et al., 2007). Our ultimate goal was to engineer a SNAP-25 (or t-SNARE) that binds synaptotagmin but no longer binds to Gβγ as a tool to test the physiological role of Gβγ interaction with SNARE complexes. To more fully investigate the determinants of interaction between Gβγ and SNAP-25, we searched for small linear sequences from SNAP-25 that would interact with Gβγ.

We used a peptide synthesizer (ResPep SL) to generate a sequential series of peptides from SNAP-25 on a membrane. This membrane was exposed to $G\beta_1\gamma_1$, washed, and then exposed to an antibody specific for Gβ and a secondary anti-

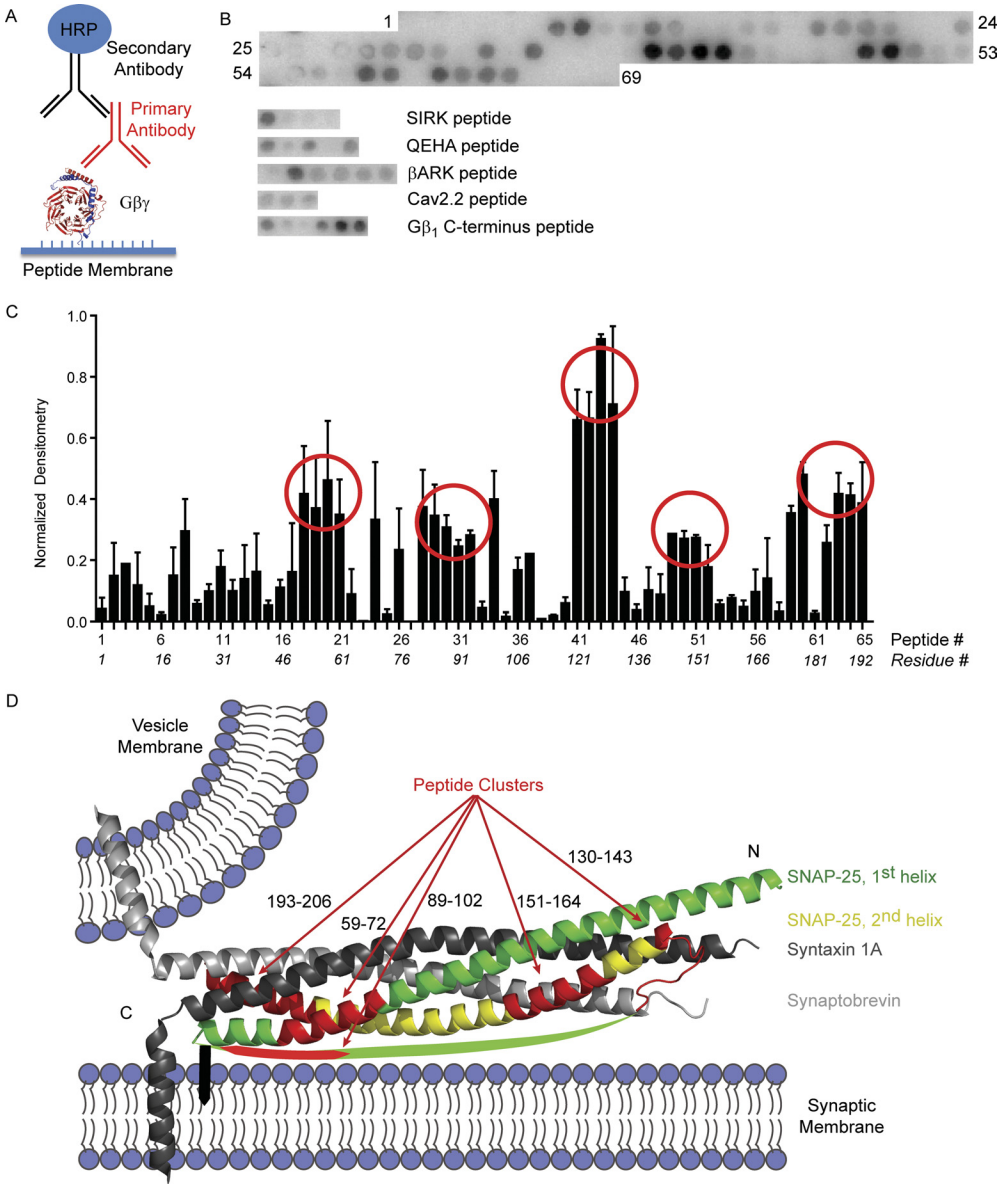

Fig. 1. Screening of SNAP-25 peptides for interaction with $G\beta_1\gamma_1$. A, the basic premise of the screening is a far-Western. The peptide synthesizer creates peptides on a derivatized membrane. With appropriate washes between steps, the membrane and peptides are sequentially exposed to $G\beta_1\gamma_1$, the primary antibody for Gβ, and horseradish peroxidase (HRP)-conjugated secondary antibody. B, representative image of a membrane exposed to $G\beta_1\gamma_1$. Numbering reflects spots with successive peptides 1 to 65. Spots 66 to 69 were left without peptide synthesized on them as negative controls. Shown separately are the peptide spots derived from the sequences for the SIRK peptide, QEHA peptide, βARK peptide, Gβγ binding domain of the calcium channel $Ca_V2.2$, and C terminus of $G\beta_1$. C, densitometry was performed on the three membranes using ImageJ analysis of the image. Each membrane was normalized to the most intense spot on the membrane. The average of the three membranes was plotted for each set of 65 peptides that span the full length of SNAP-25. The *x*-axis reflects both the peptide number according to B as well as the residue number of the first residue in each respective peptide. Circles reflect clusters of peptides with the highest densitometric signal. D, representative sequences of the clusters of SNAP-25 peptides that were found are shown in red mapped onto the representation of the X-ray crystal structure of the core SNARE motifs (PDB 1SFC). The colors signify the following: light gray; synaptobrevin; dark gray, syntaxin 1A; green, first SNAP-25 helix; yellow, second SNAP-25 helix. Syntaxin 1A and synaptobrevin each have a transmembrane domain shown as α-helices. The black bar inserted into the membrane represents the palmitoylation sites on SNAP-25. The green arc represents the nonstructured sequence between the two α-helices of SNAP-25. This arc includes one of the peptide clusters (red) near the palmitoylation site. N signifies the N-terminal end of the helices within the SNARE complex; C signifies the C-terminal end of the helices within the SNARE complex.

body that reacts in a chemiluminescent assay (Fig. 1A). Membranes consisted of 15-mer peptides shifting 3 amino acids for each successive peptide spot (1–15, 4–18, 7–21, and so on) cumulatively representing the entire sequence of SNAP-25. Membranes were made and tested in triplicate. For positive controls, peptides that were previously reported to bind G$\beta\gamma$ were spotted on the membrane [SIRK (SIRKALNILGYPDYD) (Scott et al., 2001), QEHA (QEHAQEPERQYMHIGTMVEFAYALVGK) (Weng et al., 1996), and the C terminus of βARK (WKKELRDAYREAQQLVQRVPKMKNK PRS) (Koch et al., 1993)], as well as a peptide based on the G$\beta\gamma$-binding sequence from the calcium channel $Ca_V2.2$ (GID site: KSPLDAVLKRAATKKSRNDLI) (De Waard et al., 2005). The epitope of the primary antibody, the extreme C terminus of Gβ_1, was used as a positive control. Shown in Fig. 1B is a representative image of the spotted membrane for the SNAP-25 protein and the other G$\beta\gamma$ interacting peptides, as well as the antibody-binding positive control. As can be seen from the image of the SNAP-25 peptides, there are several clusters of consecutive peptides of SNAP-25 that bind G$\beta_1\gamma_1$ (see red circles in Fig. 1B). Locations 64 to 69 on the membrane are intentionally underivatized by peptides during the synthesis to demonstrate nonspecific binding of G$\beta\gamma$ or antibodies with the membrane alone. Densitometry was performed on images of the triplicate membranes and normalized to the brightest signal for each membrane, respectively. Figure 1C is a bar graph across all 65 peptides from the sequence of SNAP-25 showing clusters of reactive peptides spanning residues 49 to 75, 82 to 108, 121 to 144, 145 to 168, and 184 to 206. The sequences in common for each cluster of peptides are visualized in Fig. 1D on the X-ray crystal structure of the ternary complex of SNAP-25, syntaxin 1A, and synaptobrevin (Sutton et al., 1998). The ternary SNARE complex is depicted in a "primed" state with a docked vesicle that has not yet fused, which is the proposed location and state that would bind G$\beta\gamma$ (Blackmer et al., 2005; Yoon et al., 2007). Note that the four helices of the SNARE complex are arranged in parallel to each other with all N termini of those helices at one end of the complex and all C termini at the opposite end. The peptide sequences of SNAP-25 that bind G$\beta\gamma$ in this experiment (shown in red) are clustered on either the N-terminal end of the ternary SNARE complex (labeled N in Fig. 1D) or the C-terminal end proximal to the transmembrane domains of ternary SNARE (labeled C in Fig. 1D).

On the basis of these results, peptides that bound G$\beta\gamma$ in this screen were then subjected to alanine-scanning mutagenesis. Full-length SNAP-25 peptides were compared with the corresponding mutagenized peptides. For each series of horizontal spots, the initial spot was the wild-type sequence of a given peptide followed by spots with a single alanine mutation in the 1st through 14th residue, individually. After the results of three independent experiments were averaged, residues were identified within the sequence that had reduced ability to bind G$\beta\gamma$ when mutated to alanine in comparison with wild-type peptide. The sequences for these peptides are listed in Table 1. The bar graphs demonstrating the average densitometry of all peptides with loss of binding in a mutant are shown in Fig. 2B. This resulted in a list of nine amino acids that had disrupted binding when mutated to alanine in their respective peptides. The resulting nine amino acids, when mapped to the crystal structure of the ternary SNARE, again show two clusters at either end of the coiled-coil helical SNARE (Fig. 2C). There is one cluster near the published interaction site at the C terminus of SNAP-25

TABLE 1

SNAP-25 peptides found in screening

SNAP-25 peptides that bound to G$\beta_1\gamma_1$ in the initial screening and had loss of binding when a residue was mutated to alanine are listed. The residues important for loss of binding is shown in boldface.

Peptide	Peptide Sequence
59–72	RIE**E**GMDQINKDMK
89–102	VCPCNKLKSS**D**AY**K**
130–143	SGGFI**RR**VTNDA**R**E
151–164	EQVSGIIGNL**R**HMA
193–206	DEANQ**R**AT**K**MLGSG

(Yoon et al., 2007), including two residues within the extreme C terminus of SNAP-25: Arg198 and Lys201. In addition to those amino acids in SNAP-25 important for peptide binding shown in the X-ray crystal structure near the C terminus of SNAP-25, there are two amino acids (Asp99 and Lys102) in the linker region between the two helices of SNAP-25 in close proximity to the palmitoylation sites of SNAP-25 (Cys85, Cys88, Cys90, and Cys92) that are not in the X-ray crystal structure, but are shown in Fig. 2C in cartoon form. Of interest, when mapped to the ternary SNARE structure, residues Gly63 and Met64 that had a significant reduction in binding when mutated to alanine in the 59 to 72 SNAP-25 peptide (Fig. 2) are buried in the interface with syntaxin 1A and synaptobrevin. Because these two residues are not expected to be accessible on the basis of the X-ray crystal structure, they were omitted from mutagenesis in studies with full-length SNAP-25 protein. Of the remaining residues, seven lose a positive charge when mutated to alanine, and the other two lose a negative charge when mutated to alanine.

Effect of Alanine Mutations in Full-Length SNAP-25. We next examined the effect of mutating the nine residues of SNAP-25 determined from the peptide screening on the interaction between full-length SNAP-25 and G$\beta\gamma$. The order of mutations was chosen primarily to start from the two residues implicated in the region previously published to be important to the G$\beta\gamma$ -t-SNARE interaction: Arg198 and Lys201 of SNAP-25 (Yoon et al., 2007) that we termed "2A" upon mutagenesis. From that, further mutations of residues in close proximity to Arg198 and Lys201 found in both helices and the loop connecting the two helices were made including: E62A/R198A/K201A ("3A"), E62A/D99A/R198A/K201A ("4A"), and E62A/D99A/K102A/R198A/K201A ("5A"). Continuing, further mutations were designed beginning at the N-terminal end of the two SNAP-25 helices. This set of mutations includes E62A/D99A/K102A/R135A/R198A/K201A ("6A"), E62A/D99A/K102A/R135A/R136A/R198A/K201A ("7A"), E62A/D99A/K102A/R135A/R136A/R142A/R198A/K201A ("8A"), and E62A/D99A/K102A/R135A/R136A/R142A/R161A/R198A/K201A ("9A"). The full set of SNAP-25 mutants is defined in Table 2.

We then used a sensitive and quantitative fluorescence assay to compare the ability of wild-type SNAP-25 and these mutated SNAP-25 proteins to bind G$\beta_1\gamma_1$. Purified G$\beta_1\gamma_1$ was labeled with MIANS, an environmentally sensitive fluorescent probe. MIANS fluorescence will increase in a local hydrophobic environment, as would be anticipated in protein-protein interaction. In Fig. 3A, 20 nM MIANS-G$\beta_1\gamma_1$ fluorescence increased when exposed to increasing amounts of wild-type SNAP-25 saturating with an EC_{50} of 0.35 μM SNAP-25. Mutations 2A to 5A display decreased affinity for G$\beta\gamma$ (Fig. 3A; Table 2). The EC_{50} for the 5A mutant is 1.2 μM.

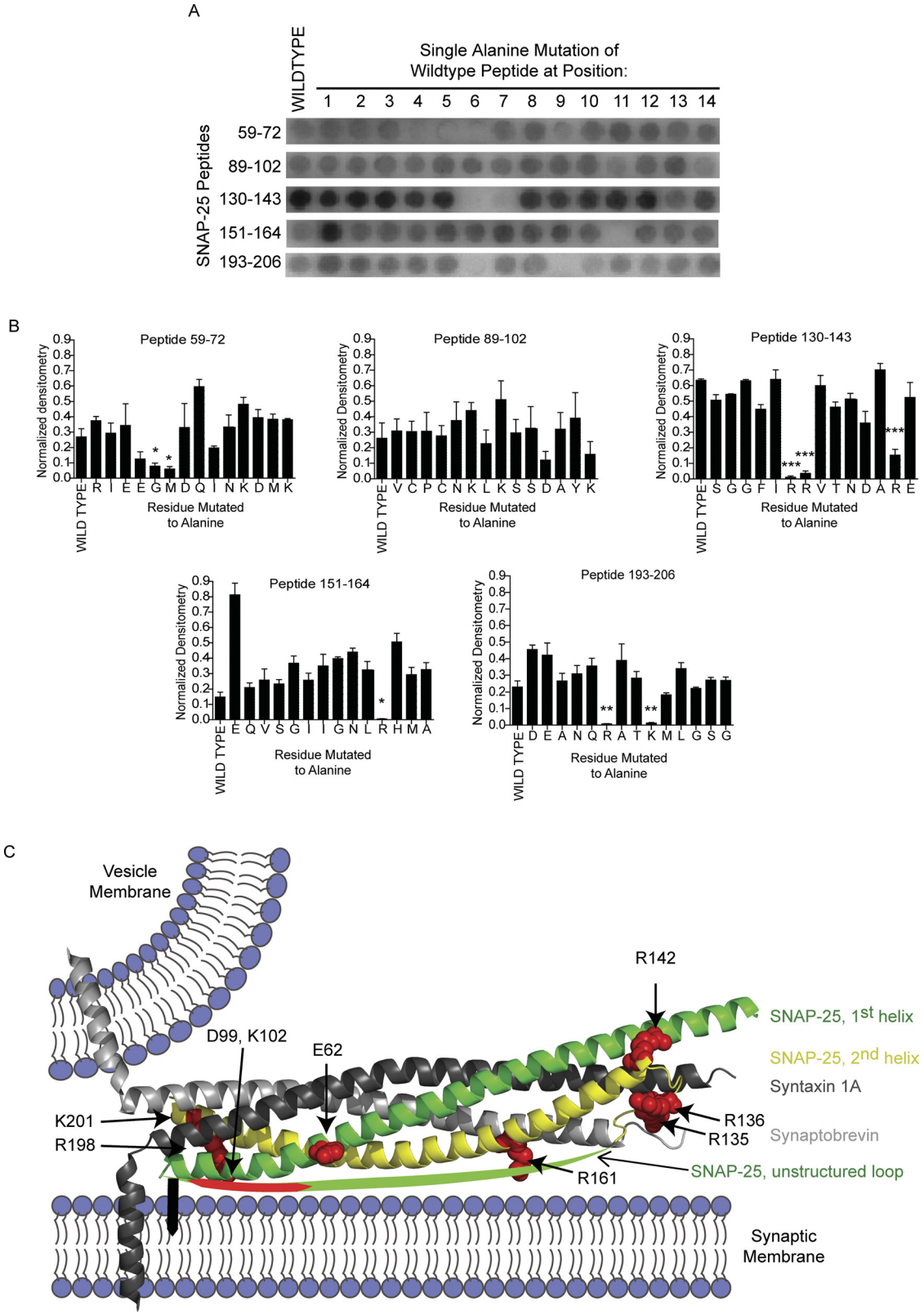

Fig. 2. Alanine mutagenesis screening of SNAP-25 peptides that bind Gβγ. A, representative image of the alanine screening for SNAP-25 peptides synthesized on a membrane. Five peptides are identified by their sequence number shown on the left. The first spot of each row contains wild-type peptide. The next 14 spots to the right are mutant peptides with a single alanine replacement of the residue at position 1, 2, 3. …, 14 for each wild-type peptide. B, densitometry was performed across three separate membranes for each respective peptide and its series of mutants. Means ± S.D. from the three membranes are shown for the five peptides in A (Student's t test; *, $p < 0.05$; **, $p < 0.01$; ***, $p < 0.001$). C, The residues (spheres, red) that had significantly reduced Gβγ binding when mutated to alanine are mapped onto the X-ray crystal structure of ternary snare (PDB 1SFC). The colors signify the following: dark gray, syntaxin 1A; light gray, synaptobrevin; green, first SNAP-25 helix; yellow, second SNAP-25 helix; green cartoon arc, unstructured domain between the two SNAP-25 α-helices.

TABLE 2

SNAP-25 alanine mutants

Residues determined to be important for G$\beta\gamma$ binding to SNAP-25 peptides were successively introduced into the native SNAP-25 sequence. Listed are the names given to each SNAP-25 mutant with the corresponding list of residues mutated to alanine. Residues in boldface are the new mutated residue added to the previously made mutant SNAP-25. Max is the maximum fluorescence enhancement (F1/F0) of the nonlinear regression for the each mutant, normalized to the maximum enhancement for wild-type SNAP-25. The N4A mutant contains only the four alanine mutations near the N terminus of the SNARE complex. Data are means (± S.E.).

Mutant Name	Residues of SNAP-25 Mutated	Log EC_{50}	EC_{50}	Max
WT	N.A.	−6.45 (± 0.20)	3.5×10^{-7}, (2.2×10^{-7}–5.6×10^{-7})	100 (± 15)
2A	R198A, K201A	−6.18 (± 0.13)	6.6×10^{-7}, (4.9×10^{-7}–8.9×10^{-7})	96 (± 10)
3A	**E62A,** R198A, K201A	−5.93 (± 0.12)	1.2×10^{-6}, (8.9×10^{-7}–1.5×10^{-6})	122 (± 16)
4A	E62A, **D99A,** R198A, K201A	−6.12 (± 0.13)	7.6×10^{-7}, (5.6×10^{-7}–1.0×10^{-6})	71 (± 8)
5A	E62A, D99A, **K102A,** R198A, K201A	−6.08 (± 0.15)	8.3×10^{-7}, (5.9×10^{-7}–1.7×10^{-6})	70 (± 9)
6A	E62A, D99A, K102A, **R135A,** R198A, K201A	−5.97 (± 0.08)	1.1×10^{-6}, (7.4×10^{-7}–1.2×10^{-6})	88 (± 8)
7A	E62A, D99A, K102A, R135A, **R136A,** R198A, K201A	−6.12 (± 0.09)	7.6×10^{-7}, (6.2×10^{-7}–8.9×10^{-7})	33 (± 3)
8A	E62A, D99A, K102A, R135A, R136A, **R142A,** R198A, K201A	−5.87 (± 0.12)	1.3×10^{-6}, (1.02×10^{-6}–1.8×10^{-6})	20 (± 3)
9A	E62A, D99A, K102A, R135A, R136A, R142A, **R161A,** R198A, K201A	−6.36 (± 0.23)	4.4×10^{-7}, (2.6×10^{-7}–7.4×10^{-7})	25 (± 4)
N4A	R135A, R136A, R142A, R161A	−6.69 (± 0.14)	2.0×10^{-7}, (1.5×10^{-7}–2.8×10^{-7})	44 (± 3)

N.A., not applicable.

The mutations 3A to 5A appeared to behave similarly in this assay. Further cumulative mutations, 6A to 9A, result in limited enhancement over baseline fluorescence of MIANS-G$\beta\gamma$ compared with the increase achieved by wild-type SNAP-25 (Fig. 3B; Table 2).

To test the importance of the N-terminal region (R135A, R136A, R142A, and R161A) alone, a construct was made that incorporated only these mutations in the SNAP-25 protein. As seen in Fig. 3C, compared with wild-type SNAP-25, this mutant (N4A) had decreased maximal fluorescence, and its EC_{50} was 0.20 μM (95% CI 0.10–0.40 μM) compared with 0.40 μM (95% CI 0.25–0.64 μM) for wild type. This suggests that an interaction between G$\beta\gamma$ and SNAP-25 is altered (loss of fluorescence enhancement), but the high-affinity C-terminal binding site is maintained.

SNAP-25 C-Terminal Peptide Inhibits SNAP-25-G$\beta\gamma$ Interaction. Mutations of full-length SNAP-25 suggested a complex binding mechanism between SNAP-25 and G$\beta\gamma$ that extends beyond the C terminus of SNAP-25. Peptides identified previously in screens synthesized and screened in the fluorescence intensity assay of 20 nM MIANS-labeled $G\beta_1\gamma_1$ with a fixed amount (0.3 μM) of SNAP-25 that gives a half-maximal response ($n = 3$) were tested for their ability to inhibit the interaction between SNAP-25 and MIANS-$G\beta_1\gamma_1$. Four of the five peptides showed no effect (Fig. 4). Only the C-terminal peptide ($SNAP\text{-}25_{193–206}$) was able to inhibit the interaction significantly. This is the same peptide that was able to functionally inhibit serotonin-mediated inhibition (via G$\beta\gamma$) in lamprey central synapses (Gerachshenko et al., 2005). A modified $SNAP\text{-}25_{193–206}$ peptide in which residues Arg198 and Lys201 were mutagenized to Ala was unable to inhibit the SNAP-25-mediated fluorescent enhancement of MIANS-$G\beta_1\gamma_1$ in the same fashion as the wild-type $SNAP\text{-}25_{193–206}$ peptide (Fig. 4). It is also possible that the other peptides adopt a conformation in solution that differs from its structure in the intact protein or tethered to a membrane.

Effect of SNAP-25 Mutations on Synaptotagmin Binding. Calcium-dependent synaptotagmin binding to t-SNARE has been shown to mediate exocytotic fusion (Brose et al., 1992; Chapman and Jahn, 1994; Geppert et al., 1994; Chapman et al., 1995; Mehta et al., 1996). To confirm that mutant SNAP-25 can still interact with synaptotagmin, the GST fusion proteins of wild-type SNAP-25 or the mutants 5A to 9A immobilized to glutathione-Sepharose beads were exposed to synaptotagmin-1 C2AB, either in the presence of the calcium chelator 2 mM EGTA or 1 mM $CaCl_2$. As can be seen in Fig. 5A), wild-type SNAP-25 is capable of binding to synaptotagmin-1 in the presence of calcium with an increase in bound synaptotagmin-1, as expected. There is no statistically significant decrease in calcium-dependent binding between the SNAP-25 mutants and synaptotagmin-1 with progressive mutation of SNAP-25 residues compared with binding to wild-type SNAP-25 (Student's t test, $p > 0.05$) (Fig. 5B).

Synaptotagmin binding to SNAP-25 and syntaxin 1A can also occur in a calcium-independent manner (Gerona et al., 2000; Mahal et al., 2002; Rickman and Davletov, 2003; Nishiki and Augustine, 2004). In the presence of 2 mM EGTA, the interaction between synaptotagmin-1 and mutant SNAP-25 (6A) (Student's t test, $p < 0.05$) and SNAP-25 (9A) (Student's t test, $p < 0.01$) is reduced relative to that of wild-type SNAP-25. Binding was most dramatically reduced for the SNAP-25 9A mutant, suggesting that that calcium-independent binding of synaptotagmin-1 to SNAP-25 is at least in part mediated by Arg161. To test this, the single mutation R161A was made in wild-type SNAP-25, and pull-down experiments were performed with synaptotagmin-1 C2AB. As can be seen in the Western blots in Fig. 5C and densitometry measurements over three separate experiments in Fig. 5D, mutation of this one residue resulted in a significant decrease in calcium-independent binding of synaptotagmin-1 compared with that of wild-type SNAP-25 (Student's t test, $p < 0.01$); however, there was no difference in calcium-dependent binding to synaptotagmin-1 between SNAP-25 and SNAP-25 (R161A). These results for SNAP-25 (R161A) are similar to the results for SNAP-25 (9A).

t-SNARE Formed with Syntaxin 1A and SNAP-25 (8A) Has Decreased Affinity for G$\beta\gamma$. We investigated whether SNAP-25 mutations would reduce $G\beta_1\gamma_1$ binding when assembled with syntaxin 1A into a t-SNARE complex. Increasing concentrations of t-SNARE consisting of full-length syntaxin 1A and SNAP-25 increased fluorescence of MIANS-$G\beta_1\gamma_1$. The EC_{50} was 0.13 μM ($n = 4$; 95% CI 0.067–0.26 μM) (Fig. 6), similar to the results shown earlier and those reported by Yoon et al. (2007). With use of a subcloning strategy, eight of the alanine mutations were introduced with a single reaction into the SNAP-25 sequence in a vector that contains both full-length syntaxin 1A and SNAP-25 that is used to dually express both proteins simultaneously to pro-

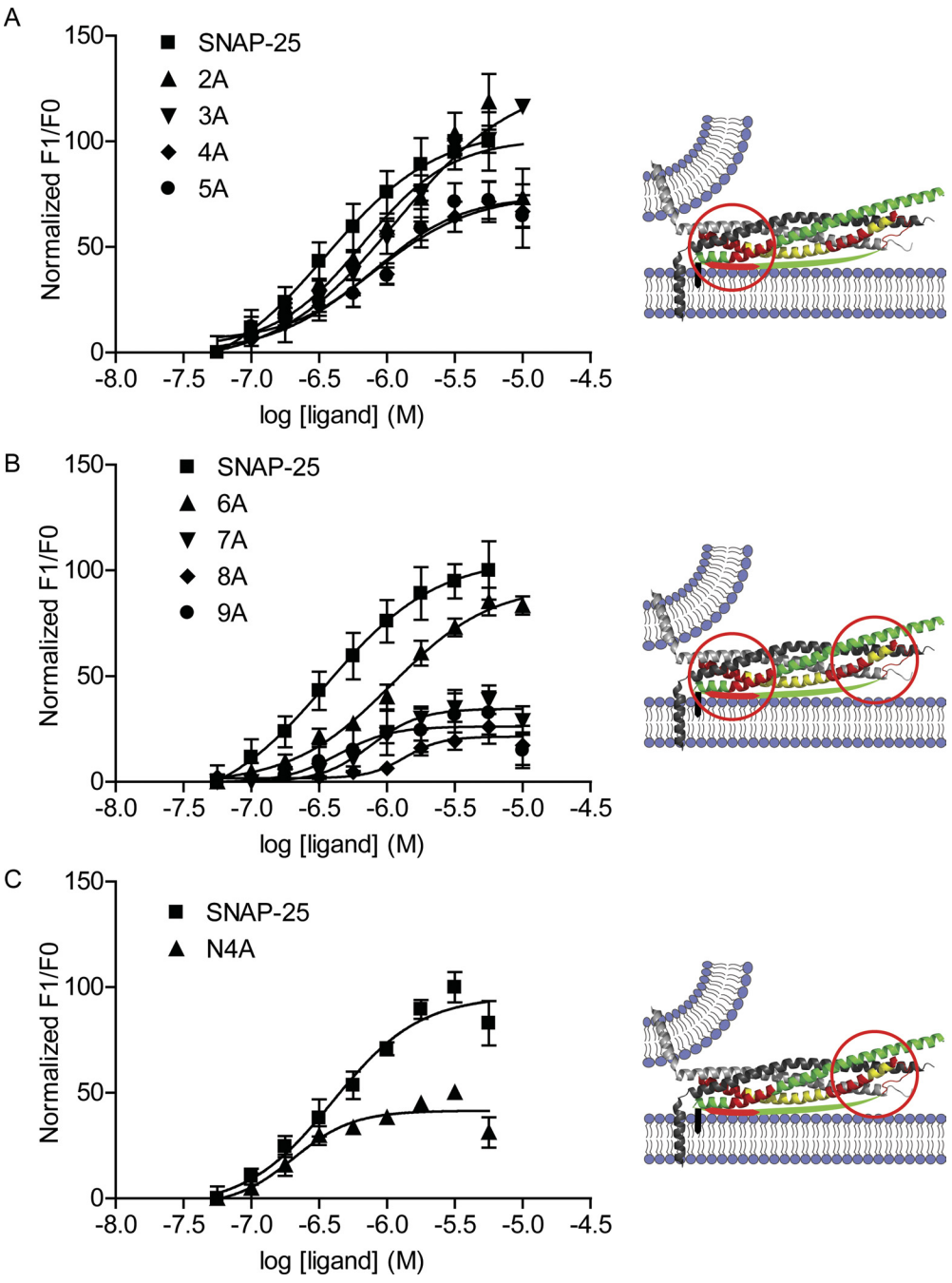

Fig. 3. Binding of SNAP-25 and its alanine mutants to MIANS-labeled Gβγ. A, a fixed concentration of MIANS-$G\beta_1\gamma_1$ (20 nM) was exposed to increasing concentrations of SNAP-25 with resulting increase in fluorescence. $n = 4$. F1/F0 is the ratio of fluorescence of $G\beta_1\gamma_1$ measured in the presence of SNAP-25 over the fluorescence of $G\beta_1\gamma_1$ in the absence of SNAP-25. The fluorescence was corrected for any intrinsic fluorescence of SNAP-25 at the various concentrations. Finally, all of the curves were normalized to the highest fluorescence achieved by binding of wild-type SNAP-25 to $G\beta_1\gamma_1$. A, dose-response curves for wild-type SNAP-25, SNAP-25 (2A), SNAP-25 (3A), SNAP-25 (4A), and SNAP-25 (5A). To the right of the dose-response curves is a cartoon modified from Fig. 2. The red circle denotes the area on the SNARE complex where these mutated residues are located together in the C terminus. B, the remaining alanine mutants of SNAP-25 were tested for binding to MIANS-$G\beta_1\gamma_1$. Compared with wild-type SNAP-25, increasing numbers of mutations resulted in decreased EC_{50} and then decreased maximum fluorescence enhancement of MIANS-$G\beta_1\gamma_1$ (A and B). C, a SNAP-25 mutant with residues in the amino-terminal region (R135A, R136A, R142A, and R161A) of the SNAP-25 protein termed N4A. When exposed to fluorescently labeled $G\beta_1\gamma_1$, this mutant (N4A) had a decreased maximal fluorescence, and its EC50 was 0.20 μM compared with 0.35 μM. The cartoon in the right portion of C shows the region with N-terminal mutated residues.

mote efficient t-SNARE formation. When t-SNARE consisting of syntaxin 1A with this subcloned SNAP-25 (8A) mutant, termed t-SNARE (8A), was used in this assay, a maximal fluorescence enhancement identical to that for wild-type t-SNARE was observed (Fig. 6), but this t-SNARE (8A) had a 4-fold lower affinity for MIANS-$G\beta_1\gamma_1$ with a measured EC_{50} of 0.58 μM ($n = 4$; 95% CI 0.47–0.70 μM).

SNARE Complexes Formed with SNAP-25 (8A) in Neurons Has Impaired Ability to Support Gβγ-Mediated Inhibition. If Gβγ inhibits exocytosis by interacting with t-SNARE, the mutant SNAP-25 that interacts less well with Gβγ should decrease the effect of Gβγ on exocytosis. To test this hypothesis, mutant SNAP-25s were injected into lamprey neurons to test its ability to impair serotonin-mediated inhibition of vesicle release, which is mediated by Gβγ (Blackmer et al., 2001; Gerachshenko et al., 2005). Synaptic responses were evoked at 30-s intervals by evoking presynaptic action potentials with brief depolarizing current pulses (2 ms, 1–3 nA). After at least 10 responses were obtained, serotonin (1 μM) was bath-applied to the preparation and a further series of EPSCs was evoked. Serotonin significantly reduced the EPSC amplitudes to 24 ± 8% of the control amplitude. SNAP-25 and SNAP-25 (8A) was injected into presynaptic axons using pressure pulses. We confirmed that SNAP-25 protein was injected by imaging injected SNAP-25 that had been fluorescently labeled in four paired cell recordings (data not shown).

We sought to replace endogenous SNAP-25 with a mutant form in the giant synapses. To facilitate this experiment, SNAP-25 was modified to be resistant to BoNT/E by mutat-

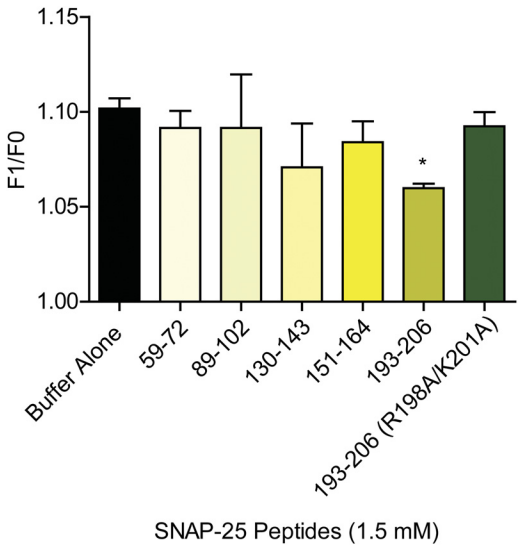

Fig. 4. Inhibition of G$\beta\gamma$-SNAP-25 binding by SNAP-25 peptides. Each peptide (1.5 mM) was added to the fluorescence assay detecting the interaction of 20 nM MIANS-G$\beta_1\gamma_1$with 0.3 μM SNAP-25. The C-terminal peptide (193–206) was the only peptide to significantly decrease the fluorescence enhancement (Student's t test, $p < 0.01$; $n = 3$). When the residues Arg198 and Lys201 were changed to alanine in that peptide, the peptide was no longer effective at reducing fluorescence enhancement by SNAP-25 (Student's t test, $p > 0.05$; $n = 3$).

ing Asp179 to Lys (Zhang et al., 2002). Either SNAP-25 (D179K) or SNAP-25 (D179K) (8A) was injected (1 mg/ml) along with light chain BoNT/E (25 μg/ml) into a presynaptic neuron in the lamprey. After the initial responses for 5 min were recorded, as well as an initial 300 stimuli at 1 Hz to remove docked and primed vesicles (Gerachshenko et al., 2005), EPSCs were recorded again after 5 min of recovery. Injection of BoNT/E alone eliminated synaptic transmission (Fig. 7A). In contrast, injection of BoNT/E together with SNAP-25 (D179K) partially restored synaptic transmission, showing that the injected SNAP-25 was capable of reconstituting t-SNAREs with endogenous syntaxin1A (Fig. 7B). Treatment with 5-HT (1 μM) inhibited synaptic transmission to 24 $\pm$ 13% control ($n = 3$), evidence that injected SNAP-25 could support the normal G$\beta\gamma$-mediated inhibition of synaptic transmission. To test whether SNAP-25 (8A) can support 5-HT-mediated presynaptic inhibition, SNAP-25 (D179K) (8A) was injected presynaptically together with BoNT/E. After a period of 300 stimuli (1 Hz), the EPSC amplitude was recovered to 73 $\pm$ 9% of control amplitude ($n = 5$) (Fig. 7C). Thus, SNAP-25 with the eight Ala mutations still interacted with the rest of the exocytotic machinery properly. Application of 5-HT had a significantly reduced effect on EPSC amplitude in the presence of SNAP-25 (D179K) (8A). This is shown by EPSC amplitudes reduced to 76 $\pm$ 5% of the amplitude before 5-HT ($p < 0.01$ compared with inhibition seen using either 5-HT alone or after injection of the protein without including BoNt/E) (Fig. 7c). This is evidence that decreasing the affinity of G$\beta\gamma$ for SNAP-25 impairs the normal function of the inhibitory 5-HT receptor to decrease synaptic transmission through the G$\beta\gamma$ subunit.

Discussion

In this study, we have defined the critical residues on SNAP-25 for G$\beta\gamma$ binding and created a SNAP-25 with minimal affinity for G$\beta\gamma$, which still interacts in a calcium-dependent manner with synaptotagmin-1. We have confirmed the previously determined C-terminal interaction (Yoon et al., 2007) as well as identified another binding site at the distal end of the coiled-coil of t-SNARE. In addition, we have shown that one of the G$\beta\gamma$-binding residues, Arg161, is involved in calcium-independent binding to synaptotagmin-1. These two clusters of residues, one at the C terminus of SNAP-25 (C domain) and a second near the N terminus of SNAP-25 (N domain), suggest a more complex interaction between G$\beta\gamma$ and SNAP-25. These data confirm the direct role of G$\beta\gamma$ regulation of synaptic vesicle release at the exocytotic machinery. SNAP-25 (8A) retains its ability to form SNARE complexes and participate in exocytosis as shown in lamprey neurons, evidence that its interactions with syntaxin, synaptobrevin, and synaptotagmin are not perturbed. The fact that 5-HT-mediated inhibition of EPSCs was dramatically attenuated by SNAP-25 (8A) even while the in vitro interaction of G$\beta\gamma$ with t-SNARE was decreased only 4-fold by this mutant confirms the previous findings of Gerachshenko et al. (2005) that SNAP-25 is critically important for the inhibition by G$\beta\gamma$ of exocytosis.

Previous work determined that the C terminus of SNAP-25 was important in the binding of G$\beta\gamma$ at the molecular level as well as in synaptic function (Blackmer et al., 2005; Gerachshenko et al., 2005; Yoon et al., 2007; Zhao et al., 2010). Functional studies showed that BoNT/A treatment eliminated the modulatory effect of the $G_{i/o}$-coupled 5-HT receptor and G$\beta\gamma$ on synaptic transmission (Gerachshenko et al., 2005). Biochemical studies showed a decrease in affinity between G$\beta_1\gamma_1$ and SNAP-25 when its C-terminal nine amino acids were removed compared with wild-type SNAP-25, but there was complete loss of binding when the C-terminal 26 amino acids were removed, suggesting that the major functional binding site of G$\beta\gamma$ was within those C-terminal 26 amino acids (Yoon et al., 2007). The ability of SNAP-25 C-terminal peptides to inhibit wild-type SNAP-25 binding to G$\beta_1\gamma_1$ confirmed the importance of the C terminus of SNAP-25 (Fig. 4). Peptides derived from the N domain did not compete with wild-type SNAP-25, reflecting the higher affinity of the C domain.

Blackmer et al. (2005) and Yoon et al. (2007) showed that G$\beta\gamma$ and synaptotagmin-1 C2AB compete for binding to t-SNARE and postulated a mechanism by which presynaptic $G_{i/o}$-coupled receptors, via G$\beta\gamma$, inhibit exocytosis. G$\beta\gamma$ binding to ternary SNARE made with SNAP-25 missing its C-terminal nine amino acids was more sensitive to competition by synaptotagmin-1 than wild-type ternary SNARE (Yoon et al., 2007). We have defined key residues in this region as Arg198 and Lys201. In addition, we discovered a set of residues that may be near this region, Asp99 and Lys102, within a loop that is unresolved in the X-ray crystal structures of SNARE complexes, as well as Glu62, in the first helix of SNAP-25 (Fig. 2). When all of these residues are mutated to Ala (5A), its apparent affinity for G$\beta\gamma$ goes from 0.35 to 0.83 μM (Fig. 3).

Our work suggests a second region on SNAP-25 important for binding G$\beta\gamma$, a region on the second helix of SNAP-25 in close proximity to its N terminus including Arg135, Arg136, and Arg142 (Fig. 8). Alanine substitution of these residues leads to slightly increased affinity (wild-type 0.40 μM compared with N4A 0.20 μM) with decreased maximal fluores-

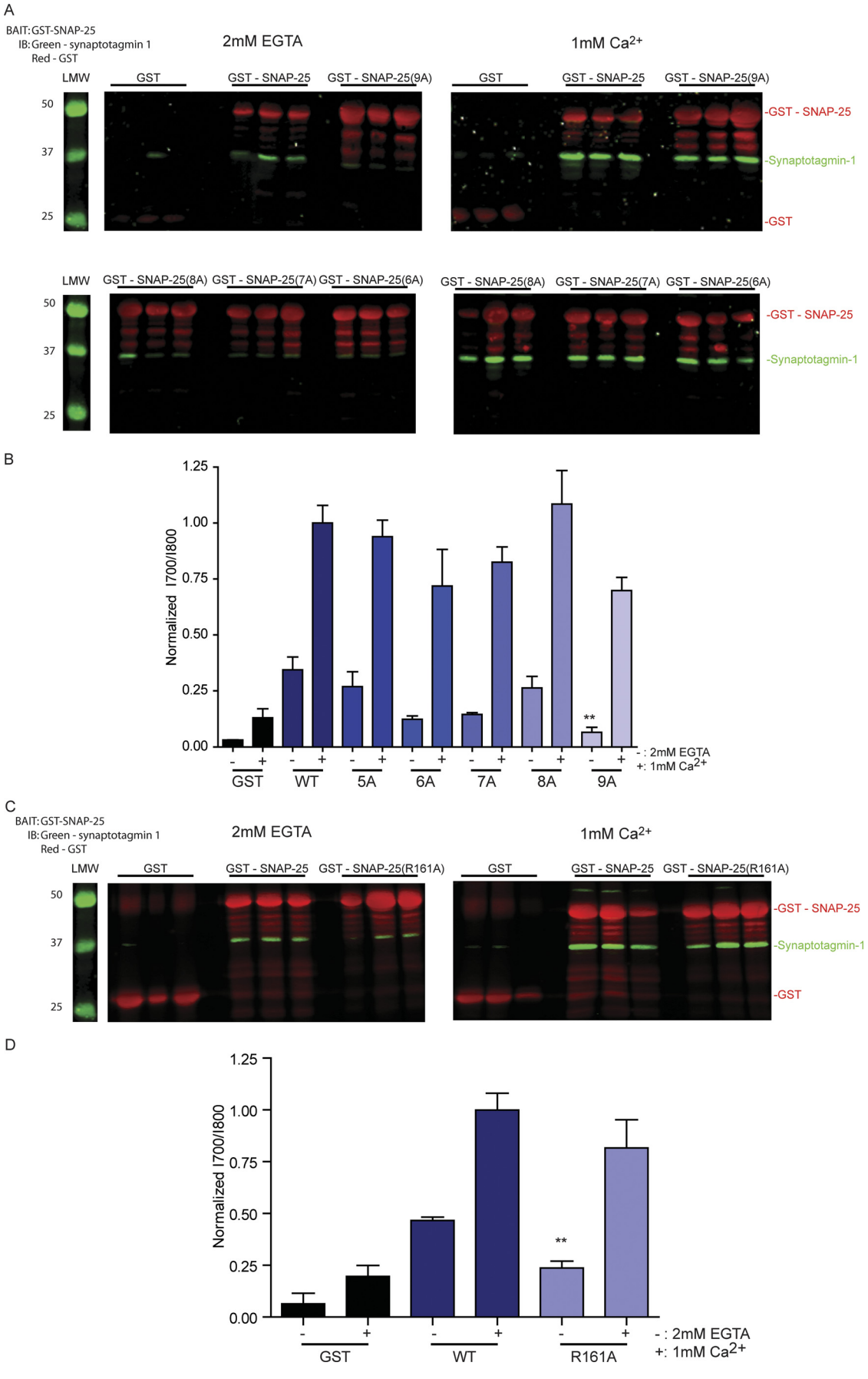
A
BAIT: GST-SNAP-25
IB: Green - synaptotagmin 1
Red - GST
2mM EGTA
1mM Ca2+
LMW
GST
GST - SNAP-25
GST - SNAP-25(9A)
50
37
25
-GST - SNAP-25
-Synaptotagmin-1
-GST
GST - SNAP-25(8A)
GST - SNAP-25(7A)
GST - SNAP-25(6A)
B
Normalized I700/I800
1.25
1.00
0.75
0.50
0.25
0.00
**
- : 2mM EGTA
+: 1mM Ca2+
GST
WT
5A
6A
7A
8A
9A
C
BAIT: GST-SNAP-25
IB: Green - synaptotagmin 1
Red - GST
2mM EGTA
1mM Ca2+
LMW
GST
GST - SNAP-25
GST - SNAP-25(R161A)
50
37
25
-GST - SNAP-25
-Synaptotagmin-1
-GST
D
Normalized I700/I800
1.25
1.00
0.75
0.50
0.25
0.00
**
- : 2mM EGTA
+: 1mM Ca2+
GST
WT
R161A

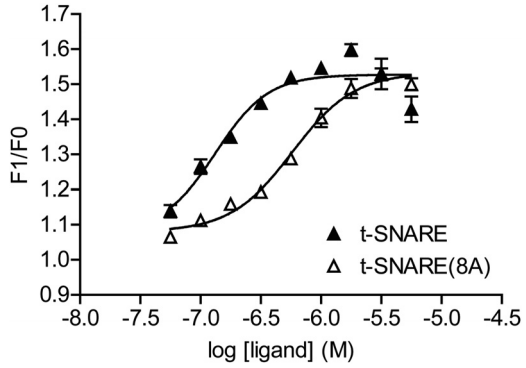

Fig. 6. Binding of wild-type t-SNARE and SNAP-25 (8A) t-SNARE to MIANS-labeled Gβγ. A fixed concentration of MIANS-$G\beta_1\gamma_1$ (20 nM) was exposed to increasing concentrations of wild-type t-SNARE with a resulting increase in fluorescence (▲, $n = 4$). The EC_{50} for t-SNARE binding to MIANS-$G\beta_1\gamma_1$ was 0.13 μM (95% CI 0.07–0.26 μM). Likewise, the t-SNARE complex of syntaxin 1A with SNAP-25 (8A) was exposed to MIANS-$G\beta_1\gamma_1$ with the resulting increase in fluorescence shown in the figure (△, $n = 4$). The EC50 for this complex binding to $G\beta_1\gamma_1$ is 0.58 μM (95% CI, 0.47–0.70 μM).

cence (Fig. 3C). Substitution of the C domain as well as the N domain residues (9A) leads to an overall decrease in EC_{50} for Gβγ and decreased maximal fluorescence.

We showed previously that the ability of Gβγ to inhibit exocytosis is overcome in high calcium (Yoon et al., 2007); we speculated that the higher affinity of Ca^{2+}-synaptotagmin for t-SNARE could overcome Gβγ competition. Remarkably, the residues on SNAP-25 that are important for Gβγ binding do not interfere with calcium-dependent binding of synaptotagmin-1 C2AB (Fig. 5). Previous studies showed three Asp residues (Asp179, Asp186, and Asp193) at the C terminus of SNAP-25 are required for calcium-dependent binding of synaptotagmin-1 to SNAP-25 (Zhang et al., 2002). It is interesting that Gβγ and Ca^{2+}-synaptotagmin-1 C2AB bind the same region of SNAP-25 but use different residues for binding this region. There is also minor calcium-independent binding of synaptotagmin-1 to t-SNARE (Gerona et al., 2000; Mahal et al., 2002; Rickman and Davletov, 2003; Nishiki and Augustine, 2004). We show that mutating Arg161 to Ala significantly decreases calcium-independent binding of synaptotagmin-1 to SNAP-25, without affecting calcium-dependent SNAP-25-synaptotagmin-1 interaction (Fig. 5).

Limited docking of Gβγ and t-SNARE structures show that these two clusters of interacting residues on SNAP-25 are too distant for binding between one dimer of Gβγ and one t-SNARE complex. By measuring the X-ray structures of ternary SNARE (PDB 1SFC) (Sutton et al., 1998) and $G\beta_1\gamma_1$ (PDB 1TBG (Sondek et al., 1996), respectively, the distance between the most distal mutated SNAP-25 residues, 135 and 201, is ~90 Å, and the greatest distance across $G\beta_1\gamma_1$ is ~70 Å. These two binding sites may permit more than one Gβγ dimer to bind a single SNARE complex (greater than 1:1 stoichiometry) whereby two separate dimers occupy the respective binding sites on a single ternary SNARE. On the basis of other known interactions of SNARE complexes with other proteins, Gβγ may shift from the high-affinity to low-affinity binding sites or vice versa in the context of simultaneous interactions. Alternatively, SNAP-25 or Gβγ may adopt conformations upon binding different from those reported in existing X-ray crystallographic structures of SNARE proteins. To date, however, no structures have been reported for Gβγ-SNARE complexes, t-SNARE alone, or t-SNARE in complex with full-length synaptobrevin during the initial stages of ternary SNARE complex formation. In the other reported structures, SNAP-25 and syntaxin 1A adopted the same conformation regardless of partner (Sutton et al., 1998; Chen et al., 2002; Pobbati et al., 2004; Kümmel et al., 2011).

When a mutated SNAP-25 was expressed and purified in the context of full-length syntaxin-1A, the t-SNARE had a reduction in affinity for Gβγ compared with wild type (Fig. 6). This result demonstrated that altering the binding affinity of SNAP-25 can change the binding affinity of the t-SNARE complex for Gβγ in the context of t-SNARE with wild-type syntaxin 1A. Furthermore, in the presence of this mutant SNAP-25, Gβγ was dramatically less effective at mediating presynaptic inhibition of vesicle release by 5-HT in lamprey neurons (Fig. 7).

The importance of the newly identified residues may be in the context of other interactions with the ternary SNARE complex. Numerous other proteins bind to SNARE proteins including calcium channels (Davies et al., 2011), Munc18 (Smyth et al., 2010), tomosyn (Hatsuzawa et al., 2003), and complexin (Tang, 2009). There is evidence of complex interactions, such as those between syntaxin 1A, Gβγ, and the calcium channel (Jarvis et al., 2000). In general, there are rearrangements thought to occur within the SNARE proteins throughout the process of regulated exocytosis. One such rearrangement is the transition of syntaxin 1A from a closed to an open position with the relative movement of the H_{abc} region away from the remainder of the complex containing the SNARE motifs (Dulubova et al., 1999; Hammarlund et al., 2007; Gerber et al., 2008). In addition, there is evidence of two states of SNARE complex: an "unzipped" state that occurs in the docking phase where there is recognition between vesicle and plasma membrane, but the vesicle is not primed and cannot fuse, and the fully "zipped" state that has full association of the SNARE motifs and is fully primed before calcium-triggered synaptotagmin-1 binding and fusion of the two membranes (Rickman and Davletov, 2003; Nishiki and Augustine, 2004; Pobbati et al., 2006; Wu et al., 2012). Our results suggest two binding sites for Gβγ and suggest

Fig. 5. Binding of SNAP-25 mutants to synaptotagmin-1 by GST pulldowns. A, GST, GST-SNAP-25 wild-type, and GST mutant SNAP-25 (6A) through SNAP-25 (9A) on glutathione beads were exposed to synaptotagmin-1 for 1 h in either 1 mM calcium or 2 mM EGTA, washed, and then eluted with sample buffer. Representative blots were imaged with Odyssey for simultaneous quantitation of synaptotagmin-1 (green) and GST (red) signal intensity. B, the ratio of normalized synaptotagmin-1: GST signals were averaged over three samples in the two conditions. The results are shown in the bar graph (**, $p < 0.01$ compared with WT in 2 mM EGTA; one-way analysis of variance, Tukey's multiple comparison post-test). C, GST, GST-SNAP-25 wild-type, and GST-fused mutant SNAP-25 (R161A) on glutathione beads were exposed to synaptotagmin-1 for 1 h in either 1 mM calcium or 2 mM EGTA, washed, and then eluted with sample buffer. Representative blots were imaged with Odyssey for simultaneous quantitation of synaptotagmin-1 (green) and GST (red) signal intensity. D, the ratio of normalized synaptotagmin-1:GST signals were averaged over three samples in the two conditions. The results are shown in the bar graph (**, $p < 0.01$ compared with WT in 2 mM EGTA; Student's t test). IB, immunoblot; LMW, low molecular weight.

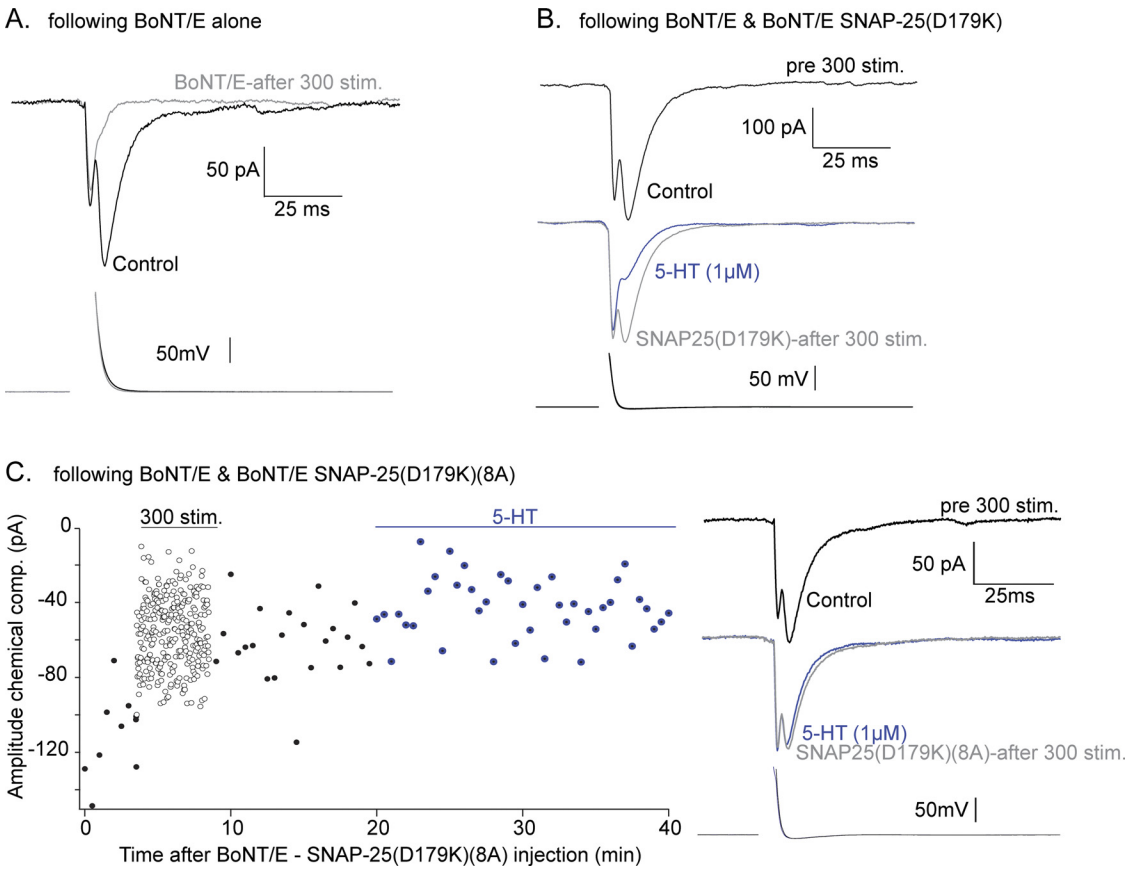

Fig. 7. Effect of SNAP-25 (8A) on presynaptic inhibition in lamprey with 5-HT. Paired cell recordings were made between lamprey giant reticulospinal axons and postsynaptic ventral horn target neurons. Each recording shown is the mean of at least 10 sequential responses. Overlaid presynaptic action potentials are shown below. A, in a recording in which BoNt/E was included in the presynaptic microelectrode, pressure injection of BoNt/E toxin left synaptic transmission intact (black). A period of 300 stimuli (1Hz) left no remaining chemical EPSC (early component is electrical) after loss of primed toxin-resistant vesicles. B, a similar recording in which BoNt/E and SNAP-25 (D179) were included in the presynaptic electrode. A period of 300 stimuli (1Hz) reduced but did not eliminate the EPSC (gray). Addition of 5-HT (1 μM) substantially reduced this remaining response (blue). C, with BoNt/E and SNAP-25 (D179) (8A) included in the presynaptic pipette. The graph shows peak chemical EPSC amplitudes recorded against time before (●) during (○) and after (●) 300 stimuli at 1Hz. Addition of 5-HT (1 μM, blue) failed to inhibit the synaptic response. EPSC examples are means of 10 from before (black), after 300 stimuli (1 Hz, gray), and after addition of 5-HT (1 μM, blue).

that Gβγ interactions with SNARE complexes could have a role in these and other interactions besides competition for binding with synaptotagmin-1 for SNARE proteins (Yoon et al., 2007). Further studies will determine whether residues identified in our studies may have implications in those systems.

The success of the peptide screening technique will allow us to similarly characterize the interaction of Gβγ with syntaxin 1A and synaptobrevin, as well as characterize the binding sites on Gβγ that interact with the SNARE complex. Further work will also be performed to explore other protein-protein interactions of the exocytotic machinery that might be affected by mutation of these eight residues on SNAP-25.

In summary, we have established novel residues on SNAP-25 for Gβγ, which implies complex binding between

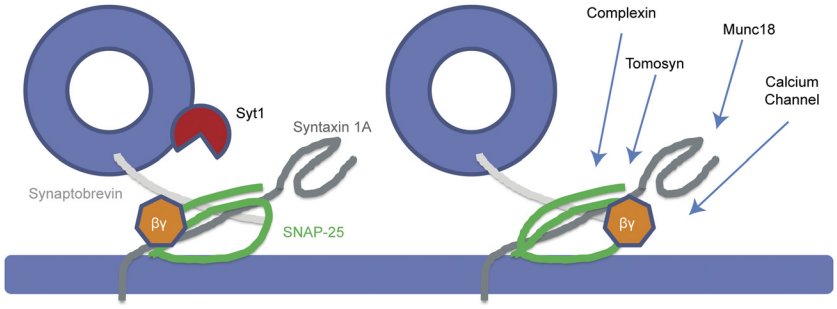

Fig. 8. Gβγ-SNARE binding model. Based on the results of this study, not only does Gβγ appear to bind at or near the C terminus of SNAP-25, but also there are additional residues distal to the membrane-approximated portion of SNAP-25. Taken in the context of ternary SNARE and its proposed position at a docked synaptic vesicle, a single Gβγ dimer activated by a $G_{i/o}$-coupled GPCR that is bound to the C terminus of SNAP-25 would not be able to bind the distal portion of the SNARE complex at the same time. The additional residues appear to have implications in calcium-independent binding of synaptotagmin, but they may also have importance for Gβγ modulation of other interactions with SNARE proteins. These could include calcium channels, tomosyn, complexin, and Munc18.

the two partners. Mutation of these residues to Ala led to a decreased affinity for G$\beta\gamma$. This allowed us to critically test the hypothesis that $G_{i/o}$-coupled 5-HT receptors cause inhibition of vesicle fusion through G$\beta\gamma$ interaction with SNARE. Mutant SNAP-25 (8A) has loss of binding to G$\beta\gamma$ but retains its ability to form SNARE complexes and participate in exocytosis, thereby confirming the direct role of G$\beta\gamma$ regulation of synaptic vesicle release at the exocytotic machinery.

Acknowledgments

We thank Nathan Swentko (Intavis) for his assistance in using the ResPepSL. We thank Summer Young (Vanderbilt) for assistance in peptide synthesis. We thank Nathan Kett (Vanderbilt) for assistance in HPLC purification of the peptides. We thank Matthew Duvernay for critical review of the manuscript. Last, we thank Ed Chapman for providing the t-SNARE dual-expression vector.

Authorship Contributions

Participated in research design: Wells, Zurawski, Betke, Alford, and Hamm.

Conducted experiments: Wells, Zurawski, Betke, Yim, Rodriguez, and Alford.

Performed data analysis: Wells, Zurawski, and Alford.

Wrote or contributed to the writing of the manuscript: Wells, Zurawski, Alford, and Hamm.

References

Betke KM, Wells CA, and Hamm HE (2012) GPCR mediated regulation of synaptic transmission. *Prog Neurobiol* **96:**304–321.

Binz T, Blasi J, Yamasaki S, Baumeister A, Link E, Südhof TC, Jahn R, and Niemann H (1994) Proteolysis of SNAP-25 by types E and A botulinal neurotoxins. *J Biol Chem* **269:**1617–1620.

Blackmer T, Larsen EC, Bartleson C, Kowalchyk JA, Yoon EJ, Preininger AM, Alford S, Hamm HE, and Martin TF (2005) G protein $\beta\gamma$ directly regulates SNARE protein fusion machinery for secretory granule exocytosis. *Nat Neurosci* **8:**421–425.

Blackmer T, Larsen EC, Takahashi M, Martin TF, Alford S, and Hamm HE (2001) G protein $\beta\gamma$ subunit-mediated presynaptic inhibition: regulation of exocytotic fusion downstream of Ca^{2+} entry. *Science* 292:293–297.

Brose N, Petrenko AG, Südhof TC, and Jahn R (1992) Synaptotagmin—a calcium sensor on the synaptic vesicle surface. *Science* 256(5059):1021–1025.

Cabrera-Vera TM, Vanhauwe J, Thomas TO, Medkova M, Preininger A, Mazzoni MR, and Hamm HE (2003) Insights into G protein structure, function, and regulation. *Endocr Rev* **24:**765–781.

Chapman ER, Hanson PI, An S, and Jahn R (1995) Ca^{2+} regulates the interaction between synaptotagmin and syntaxin 1. *J Biol Chem* **270:**23667–23671.

Chapman ER and Jahn R (1994) Calcium-dependent interaction of the cytoplasmic region of synaptotagmin with membranes—autonomous function of a single C2-homologous domain. *J Biol Chem* **269:**5735–5741.

Chen X, Tomchick DR, Kovrigin E, Araç D, Machius M, Südhof TC, and Rizo J (2002) Three-dimensional structure of the complexin/SNARE complex. *Neuron* **33:**397–409.

Chicka MC, Hui E, Liu H, and Chapman ER (2008) Synaptotagmin arrests the SNARE complex before triggering fast, efficient membrane fusion in response to Ca^{2+}. *Nat Struct Mol Biol* **15:**827–835.

Clapham DE and Neer EJ (1997) G protein $\beta\gamma$ subunits. *Annu Rev Pharmacol Toxicol* **37:**167–203.

Davies JN, Jarvis SE, and Zamponi GW (2011) Bipartite syntaxin 1A interactions mediate $Ca_V2.2$ calcium channel regulation. *Biochem Biophys Res Commun* **411:**562–568.

Delaney AJ, Crane JW, and Sah P (2007) Noradrenaline modulates transmission at a central synapse by a presynaptic mechanism. *Neuron* **56:**880–892.

De Waard M, Hering J, Weiss N, and Feltz A (2005) How do G proteins directly control neuronal Ca^{2+} channel function? *Trends Pharmacol Sci* **26:**427–436.

Dolphin AC (2003) G protein modulation of voltage-gated calcium channels. *Pharmacol Rev* **55:**607–627.

Dulubova I, Sugita S, Hill S, Hosaka M, Fernandez I, Südhof TC, and Rizo J (1999) A conformational switch in syntaxin during exocytosis: role of munc18. *EMBO J* **18:**4372–4382.

Eaton WW, Martins SS, Nestadt G, Bienvenu OJ, Clarke D, and Alexandre P (2008) The burden of mental disorders. *Epidemiol Rev* **30:**1–14.

Frank R (2002) The SPOT-synthesis technique. Synthetic peptide arrays on membrane supports—principles and applications. *J Immunol Methods* **267:**13–26.

Gautam N, Downes GB, Yan K, and Kisselev O (1998) The G-protein $\beta\gamma$ complex. *Cell Signal* **10:**447–455.

Geppert M, Goda Y, Hammer RE, Li C, Rosahl TW, Stevens CF, and Südhof TC (1994) Synaptotagmin I: a major Ca^{2+} sensor for transmitter release at a central synapse. *Cell* **79:**717–727.

Gerachshenko T, Blackmer T, Yoon EJ, Bartleson C, Hamm HE, and Alford S (2005) G$\beta\gamma$ acts at the C terminus of SNAP-25 to mediate presynaptic inhibition. *Nat Neurosci* **8:**597–605.

Gerber SH, Rah JC, Min SW, Liu X, de Wit H, Dulubova I, Meyer AC, Rizo J, Arancillo M, Hammer RE, et al. (2008) Conformational switch of syntaxin-1 controls synaptic vesicle fusion. *Science* **321:**1507–1510.

Gerona RR, Larsen EC, Kowalchyk JA, and Martin TF (2000) The C terminus of SNAP25 is essential for Ca^{2+}-dependent binding of synaptotagmin to SNARE complexes. *J Biol Chem* **275:**6328–6336.

Hammarlund M, Palfreyman MT, Watanabe S, Olsen S, and Jorgensen EM (2007) Open syntaxin docks synaptic vesicles. *PLoS Biol* **5:**e198.

Hatsuzawa K, Lang T, Fasshauer D, Bruns D, and Jahn R (2003) The R-SNARE motif of tomosyn forms SNARE core complexes with syntaxin 1 and SNAP-25 and down-regulates exocytosis. *J Biol Chem* **278:**31159–31166.

Hille B (1994) Modulation of ion-channel function by G-protein-coupled receptors. *Trends Neurosci* **17:**531–536.

Ikeda SR and Dunlap K (1999) Voltage-dependent modulation of N-type calcium channels: role of G protein subunits. *Adv Second Messenger Phosphoprotein Res* **33:**131–151.

Jarvis SE, Magga JM, Beedle AM, Braun JE, and Zamponi GW (2000) G protein modulation of N-type calcium channels is facilitated by physical interactions between syntaxin 1A and G $\beta\gamma$. *J Biol Chem* **275:**6388–6394.

Koch WJ, Inglese J, Stone WC, and Lefkowitz RJ (1993) The binding site for the $\beta\gamma$ subunits of heterotrimeric G proteins on the β-adrenergic receptor kinase. *J Biol Chem* **268:**8256–8260.

Kümmel D, Krishnakumar SS, Radoff DT, Li F, Giraudo CG, Pincet F, Rothman JE, and Reinisch KM (2011) Complexin cross-links prefusion SNAREs into a zigzag array. *Nat Struct Mol Biol* **18:**927–933.

Mahal LK, Sequeira SM, Gureasko JM, and Söllner TH (2002) Calcium-independent stimulation of membrane fusion and SNAREpin formation by synaptotagmin I. *J Cell Biol* **158:**273–282.

Mazzoni MR, Malinski JA, and Hamm HE (1991) Structural analysis of rod GTP-binding protein, Gt. Limited proteolytic digestion pattern of Gt with four proteases defines monoclonal antibody epitope. *J Biol Chem* **266:**14072–14081.

Mehta PP, Battenberg E, and Wilson MC (1996) SNAP-25 and synaptotagmin involvement in the final Ca^{2+}-dependent triggering of neurotransmitter exocytosis. *Proc Natl Acad Sci USA* **93:**10471–10476.

Nishiki T and Augustine GJ (2004) Dual roles of the C2B domain of synaptotagmin I in synchronizing Ca^{2+}-dependent neurotransmitter release. *J Neurosci* **24:**8542–8550.

Phillips WJ and Cerione RA (1991) Labeling of the $\beta\gamma$ subunit complex of transducin with an environmentally sensitive cysteine reagent. Use of fluorescence spectroscopy to monitor transducin subunit interactions. *J Biol Chem* **266:**11017–11024.

Photowala H, Blackmer T, Schwartz E, Hamm HE, and Alford S (2006) G protein $\beta\gamma$-subunits activated by serotonin mediate presynaptic inhibition by regulating vesicle fusion properties. *Proc Natl Acad Sci USA* **103:**4281–4286.

Pobbati AV, Razeto A, Böddener M, Becker S, and Fasshauer D (2004) Structural basis for the inhibitory role of tomosyn in exocytosis. *J Biol Chem* **279:**47192–47200.

Pobbati AV, Stein A, and Fasshauer D (2006) N- to C-terminal SNARE complex assembly promotes rapid membrane fusion. *Science* **313:**673–676.

Rickman C and Davletov B (2003) Mechanism of calcium-independent synaptotagmin binding to target SNAREs. *J Biol Chem* **278:**5501–5504.

Schiavo G, Santucci A, Dasgupta BR, Mehta PP, Jontes J, Benfenati F, Wilson MC, and Montecucco C (1993) Botulinum neurotoxins serotypes A and E cleave SNAP-25 at distinct COOH-terminal peptide bonds. *FEBS Lett* **335:**99–103.

Schrödinger (2010) *The PyMOL Molecular Graphics System*, version 0.99rc6, Schrödinger, LLC, Portland, OR.

Scott JK, Huang SF, Gangadhar BP, Samoriski GM, Clapp P, Gross RA, Taussig R, and Smrcka AV (2001) Evidence that a protein-protein interaction 'hot spot' on heterotrimeric G protein $\beta\gamma$ subunits is used for recognition of a subclass of effectors. *EMBO J* **20:**767–776.

Smrcka AV (2008) G protein $\beta\gamma$ subunits: central mediators of G protein-coupled receptor signaling. *Cell Mol Life Sci* **65:**2191–2214.

Smyth AM, Duncan RR, and Rickman C (2010) Munc18–1 and Syntaxin1: unraveling the interactions between the dynamic duo. *Cell Mol Neurobiol* **30:**1309–1313.

Sondek J, Bohm A, Lambright DG, Hamm HE, and Sigler PB (1996) Crystal structure of a G-protein $\beta\gamma$ dimer at 2.1A resolution. *Nature* **379:**369–374.

Sutton RB, Fasshauer D, Jahn R, and Brunger AT (1998) Crystal structure of a SNARE complex involved in synaptic exocytosis at 2.4A resolution. *Nature* **395:**347–353.

Tang J (2009) Complexins, in *Encyclopedia of Neuroscience* (Larry RS ed) pp 1–7, Academic Press, Oxford.

Tucker WC, Weber T, and Chapman ER (2004) Reconstitution of Ca^{2+}-regulated membrane fusion by synaptotagmin and SNAREs. *Science* **304:**435–438.

Vanderbeld B and Kelly GM (2000) New thoughts on the role of the beta-gamma subunit in G-protein signal transduction. *Biochem Cell Biol* **78:**537–550.

Weng G, Li J, Dingus J, Hildebrandt JD, Weinstein H, and Iyengar R (1996) Gβ subunit interacts with a peptide encoding region 956–982 of adenylyl cyclase 2. Cross-linking of the peptide to free G$\beta\gamma$ but not the heterotrimer. *J Biol Chem* **271:**26445–26448.

Wu D, Hu Q, Yan Z, Chen W, Yan C, Huang X, Zhang J, Yang P, Deng H, Wang J, et al. (2012) Structural basis of ultraviolet-B perception by UVR8. *Nature* **484:**214–219.

Yoon EJ, Gerachshenko T, Spiegelberg BD, Alford S, and Hamm HE (2007) G$\beta\gamma$ interferes with Ca^{2+}-dependent binding of synaptotagmin to the soluble *N*-ethylmaleimide-sensitive factor attachment protein receptor (SNARE) complex. *Mol Pharmacol* **72:**1210–1219.

Yoon EJ, Hamm HE, and Currie KP (2008) G protein $\beta\gamma$ subunits modulate the

number and nature of exocytotic fusion events in adrenal chromaffin cells independent of calcium entry. *J Neurophysiol* **100:**2929–2939.
Zhang XL, Upreti C, and Stanton PK (2011) Gβγ and the C terminus of SNAP-25 are necessary for long-term depression of transmitter release. *PLoS One* **6:**e20500.
Zhang X, Kim-Miller MJ, Fukuda M, Kowalchyk JA, and Martin TF (2002) Ca^{2+}-dependent synaptotagmin binding to SNAP-25 is essential for Ca^{2+}-triggered exocytosis. *Neuron* **34:**599–611.
Zhao Y, Fang Q, Straub SG, Lindau M, and Sharp GW (2010) Noradrenaline inhibits exocytosis via the G protein βγ subunit and refilling of the readily releasable granule pool via the $\alpha_{i1/2}$ subunit. *J Physiol* **588:**3485–3498.

Address correspondence to: Dr. Heidi E. Hamm, Department of Pharmacology, Vanderbilt University Medical Center, 442 Robinson Research Building, 23rd Ave. South @ Pierce, Nashville, TN 37232-6600. E-mail: heidi.hamm@vanderbilt.edu